



HAL
open science

Gravity anomalies and orthogonal box fold development on heterogeneous basement in the Neogene Ronda Depression (Western Betic Cordillera)

A. Ruiz-Constán, J. Galindo-Zaldívar, A. Pedrera, C. Sanz de Galdeano

► **To cite this version:**

A. Ruiz-Constán, J. Galindo-Zaldívar, A. Pedrera, C. Sanz de Galdeano. Gravity anomalies and orthogonal box fold development on heterogeneous basement in the Neogene Ronda Depression (Western Betic Cordillera). *Journal of Geodynamics*, 2009, 47 (4), pp.210. <10.1016/j.jog.2008.09.004>. <hal-00531894>

HAL Id: hal-00531894

<https://hal.science/hal-00531894v1>

Submitted on 4 Nov 2010

HAL is a multi-disciplinary open access archive for the deposit and dissemination of scientific research documents, whether they are published or not. The documents may come from teaching and research institutions in France or abroad, or from public or private research centers.

L'archive ouverte pluridisciplinaire **HAL**, est destinée au dépôt et à la diffusion de documents scientifiques de niveau recherche, publiés ou non, émanant des établissements d'enseignement et de recherche français ou étrangers, des laboratoires publics ou privés.

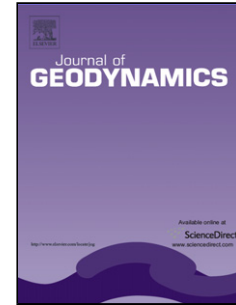


HAL Authorization

Accepted Manuscript

Title: Gravity anomalies and orthogonal box fold development on heterogeneous basement in the Neogene Ronda Depression (Western Betic Cordillera)

Authors: A. Ruiz-Constán, J. Galindo-Zaldívar, A. Pedrera, C. Sanz de Galdeano



PII: S0264-3707(08)00081-1
DOI: doi:10.1016/j.jog.2008.09.004
Reference: GEOD 868

To appear in: *Journal of Geodynamics*

Received date: 25-4-2008
Revised date: 15-9-2008
Accepted date: 15-9-2008

Please cite this article as: Ruiz-Constán, A., Galindo-Zaldívar, J., Pedrera, A., de Galdeano, C.S., Gravity anomalies and orthogonal box fold development on heterogeneous basement in the Neogene Ronda Depression (Western Betic Cordillera), *Journal of Geodynamics* (2008), doi:10.1016/j.jog.2008.09.004

This is a PDF file of an unedited manuscript that has been accepted for publication. As a service to our customers we are providing this early version of the manuscript. The manuscript will undergo copyediting, typesetting, and review of the resulting proof before it is published in its final form. Please note that during the production process errors may be discovered which could affect the content, and all legal disclaimers that apply to the journal pertain.

1 **Gravity anomalies and orthogonal box fold development on heterogeneous**
2 **basement in the Neogene Ronda Depression (Western Betic Cordillera)**

3
4 A. Ruiz-Constán^a, J. Galindo-Zaldívar^{a, b}, A. Pedrera^a and C. Sanz de Galdeano^b

5
6 a Departamento de Geodinámica. Universidad de Granada. Campus Fuentenueva,
7 18071 Granada, Spain. aconstan@ugr.es

8 b Instituto Andaluz de Ciencias de la Tierra CSIC-UGR. Facultad de Ciencias.
9 Universidad de Granada. 18071 Granada, Spain.

10
11 Abstract:

12 The Ronda Depression constitutes a Neogene intramontane basin located in the
13 External Zones of the Western Betic Cordillera. Major deformation structures affect
14 only the southwestern part of its sedimentary infill and consist of NNE-SSW and
15 WNW-ESE box folds that developed simultaneously. New gravity data reveal two
16 negative NNE-SSW elongated Bouguer anomalies, unrelated to basin depocenters, but
17 corresponding to the accumulation of low-density ductile Triassic basement rocks in the
18 core of antiforms or directly under the northwestern undeformed sedimentary infill. The
19 Subbetic basement is also deformed by Early Burdigalian to Serravallian NNE-SSW
20 folds and thrusts, although there is no clear continuity with those affecting the Late
21 Miocene sedimentary infill. The aim of this contribution is to describe in detail the Late
22 Miocene folds that deform the Ronda Depression, as well as to discuss the role of the
23 basement nature on their reactivation. The reactivation of the pre-Tortonian folds, due to
24 the heterogeneous distribution of evaporitic Triassic rocks in the basement as well as the

25 presence of rigid limestones on the southwestern basin boundary, determined the
26 simultaneous orthogonal fold development that only evidence local deformation.

27

28 Key words: Neogene basin, gravity models, low density basement, fold reactivation.

29

30 INTRODUCTION

31 The behaviour of ductile rocks facilitates the presence of detachment levels
32 determining the style of deformation. Analogue modelling studies have focused on the
33 effects of different rheological rock properties in detachment features (Nilforoushan and
34 Koyi, 2007). Anomalous evaporitic rock accumulations located in these detachments
35 greatly condition antiform nucleation (Bonini et al., 2003; Marques, 2006) and may
36 favour the simultaneous development of oblique compressive structures, sometimes
37 even orthogonal to the main structural trend (Callot et al., 2007; Crespo-Blanc, 2008).
38 Such oblique folds and thrusts have usually been interpreted as a consequence of
39 overprinted deformation stages (Caritg et al., 2003; Mon et al., 2005). Moreover, the
40 accumulation of low-density evaporitic rocks at depth determines the development of
41 vertical movements related to salt tectonics producing diapiric structures. These may be
42 isometric or elongated, depending on the origin, evolution and initial distribution of low
43 density rocks. Establishing the position of these low density evaporitic rock
44 accumulations is essential for understanding the superficial folded structures. Gravity is
45 a key for elucidating the position and geometry of such structures because they
46 commonly give rise to a negative Bouguer gravity anomaly (Jallouli et al., 2005; Pinto
47 et al., 2005).

48 Gravity studies in sedimentary basins also allow determining the thickness of the
49 sedimentary infill, related to irregularities of the basal unconformity and the presence of
50 recent deformation structures. In sedimentary basins, Bouguer anomaly minima are

51 generally interpreted as depocenters, considering that basement rocks are denser than
52 the sedimentary infill. However, in basins with heterogeneous basements, the
53 superposed effect of basement and infill rocks may give rise to a complex Bouguer
54 anomaly pattern that needs to be more fully analysed in order to isolate each
55 contribution.

56 The External Zones of the Betic Cordillera (Fig. 1) are composed of Mesozoic
57 sediments with Triassic evaporitic rocks in the lower part of the sequence. In the
58 westernmost sectors, these Mesozoic rocks are deformed mainly by NE-SW to NNE-
59 SSW folds and thrusts rooted in the evaporitic rocks. However, fold and thrust trends
60 change frequently along the Cordillera; and interference structures have been
61 recognized, as in the eastern Betics (Sanz de Galdeano et al., 2006; García-Tortosa et
62 al., 2007) and the central Betics (Crespo-Blanc, 2008). In any case, their simultaneous
63 development is still under debate because in areas like the External Zones of the Central
64 Betics, paleomagnetic studies (Platzman, 1992; Platt et al., 1995) have demonstrated a
65 late rotation, suggesting a constant initial fold orientation. In many cases, establishing
66 the age of deformation is complicated by the absence of a young sedimentary cover that
67 could be used as a marker.

68 The study of folds in Neogene-Quaternary basins allows us to characterize the
69 recent tectonic evolution simultaneous to relief uplift. Therefore, many research efforts
70 have been undertaken in the eastern (Groupe de Recherche Neotectonique de l'Arc de
71 Gibraltar, 1977; Marín-Lechado et al., 2007; Pedrera et al., 2007) and central (Ruano et
72 al. 2004) part of the Cordillera. In addition, gravimetry has been widely used in the
73 Eastern Betic Cordillera (Granada Depression, Morales et al., 1990; Campo de Dalías,
74 Marín-Lechado et al., 2007) and in the Guadix-Baza Depression (Sanz de Galdeano et
75 al., 2007) in order to determine sediment thickness distribution in Neogene-Quaternary

76 basins. However, no detailed tectonic or gravimetric research has been reported to date
77 on the intramontane sedimentary basins of Western Betics.

78 The Tortonian–Messinian Ronda Depression, located in the External Zone of the
79 Betic Cordillera, constitutes a good example of an intramontane depression that can
80 provide new insights into the development of recent deformation consisting mainly of
81 medium to large scale folds, and very scarce meso and microfaults. The aim of this
82 contribution is to describe in detail the Late Miocene folds that deform its sedimentary
83 infill, as well as their relationship with the heterogeneous pre-Miocene basement
84 structure. New gravity data acquired for this study determine the distribution of
85 evaporitic rocks below the sedimentary infill, and allow us to discuss the role of their
86 distribution on the reactivation of basement antiforms that affect the Neogene infill.

87

88 GEOLOGICAL SETTING

89 The Betic-Rif Cordillera (Fig. 1) is an arc-shaped orogen that constitutes the
90 western end of the Mediterranean Alpine chain. The outer arc of this orogen consists of
91 a fold-and-thrust belt (External Zones), while the inner arc is composed of an
92 allochthonous pile of tectonic complexes including metamorphic rocks (Internal Zones).
93 The External Zones comprise the Subbetic and Prebetic zones, the latter outcropping
94 only in the eastern Betic Cordillera. The Internal Zones are formed by three main
95 complexes that are, from bottom to top: the Nevado-Filábride (outcropping only in the
96 Eastern and Central Betics), the Alpujarride and the Maláguide complexes. In addition,
97 the Dorsal and Predorsal complexes may be located in an intermediate position, in-
98 between the Flysch Units and other units of the Internal Zones.

99 The Betic-Rif arc geometry developed during the latest Oligocene and Early to
100 Middle Miocene as a result of the Eurasian-African plate convergence and the westward

101 drift of the Internal Zones. In the Western Betic Cordillera, this setting caused the
102 northwestward thrusting and folding of the Mesozoic–Cenozoic rocks of the Subbetic
103 Units in front of the migrating Internal Zones.

104 Since the Miocene, sedimentary basins were individualised and record the
105 transition from marine to continental sedimentation as a consequence of relief uplift.
106 Deposition in the External Zones mainly took place in the Guadalquivir foreland basin
107 (Sanz de Galdeano and Vera, 1992; Viseras et al., 2004), and was conditioned by huge
108 olistostromic masses from the frontal part of the External Zones. At the beginning of the
109 Late Miocene, several piggy-back basins were individualized from the Guadalquivir
110 foreland basin (Sanz de Galdeano and Vera, 1992), during the development of the
111 Subbetic fold and thrust belt (Roldán-García, 1995; Ruano et al., 2004; Crespo-Blanc,
112 2007), with different sedimentary and tectonic signatures, due to the northwestward
113 progression of their mobile basement.

114 The Ronda Depression (Fig. 1) constitutes one of the largest piggy-back basins
115 in the Western Betics. It is located over the northwesternmost Subbetic Units with
116 continuous structure, the Subbetic Chaotic Complexes and the Flysch Units. Subbetic
117 Units are formed by Triassic to Middle Miocene sedimentary rocks with local
118 intercalations of igneous rocks. The Subbetic structure in this region is described by
119 Crespo-Blanc and Campos (2001) as a NW-vergent fold-and-thrust belt, post-Early
120 Burdigalian in age. Within the Betic External Zones, Keuper Triassic levels have been
121 traditionally considered as detachment levels where the main thrust structures are
122 generally rooted.

123 Towards the northwestern mountain front of the cordillera, Subbetic Units are
124 widely deformed and show a chaotic structure (Pérez-López and Sanz de Galdeano,
125 1994). These Subbetic Chaotic Complexes are mainly composed of a Keuper Triassic

126 matrix including post-Triassic blocks, some of them of Middle Miocene age, deformed
127 by the combined development of thrusts, slides, transcurrent faults and diapirism
128 (López-Garrido and Vera, 1974; Calaforra and Pulido-Bosch, 1999; Pérez-López and
129 Pérez-Valera, 2003).

130 Flysch Units crop out in the Betic Cordillera lengthwise along the contact
131 between the Internal and External Zones, mainly in the broad area of the Campo de
132 Gibraltar, and between the different Subbetic Units. The Mesozoic and Cenozoic
133 sediments that constitute these units are turbiditic clays and marls.

134 The sedimentary infill of the Ronda Depression (Fig.2), Late Miocene in age, is
135 divided into four formations (Serrano, 1979; Rodríguez-Fernández, 1982). From bottom
136 to top these are: I) Gastor Formation, made up of sands, silts and heterogeneous
137 conglomerates of Tortonian age that lie unconformably over the Triassic basement
138 rocks in the northwestern border of the depression. II) Tajo Formation, formed by
139 heterogeneous conglomerates of pre-Late Tortonian age with clasts sourced from the
140 Subbetic and Flysch southern units. This formation lies unconformably over the Flysch
141 Units. III) Mina Formation, located conformably over the Gastor Formation and
142 composed of marls and sandy silts of Early Tortonian-Late Messinian age. It crops out
143 in the western half of the depression. IV) Setenil Formation, Late Tortonian-Late
144 Messinian in age, cropping out throughout the depression, except in the northwestern
145 part. It lies over basement rocks or Mina Formation sediments, although it could also be
146 in facies transition with this formation. Rodríguez-Fernández (1982) differentiated two
147 members in this formation: a Limestone Member and a Calcarenite Member.

148 The Neogene sedimentary infill of the Ronda Depression lies unconformably
149 upon the External Zones and Flysch basement. The boundaries of the depression are not
150 conditioned by high angle faults such as those for many other basins of the Betic

151 Cordillera, like the Granada Basin (Rodríguez-Fernández and Sanz de Galdeano, 2006).
152 Only locally inside the Ronda Depression can we find NE-SW and NNW-SSE minor
153 normal faults, which do not reach cartographic scale. These brittle structures mainly
154 deform the Tortonian calcarenites of the Setenil formation and are concentrated in the
155 southern part of the basin.

156

157 ORTHOGONAL FOLDS IN THE RONDA DEPRESSION

158 The Neogene sediments of the Ronda Depression are deformed mainly by two
159 sets of NNE-SSW and WNW-ESE kilometre scale folds (Fig. 2). These structures have
160 a heterogeneous pattern of distribution and are mainly located in the southern and
161 southwestern parts of the Depression. In the eastern sector, outcrops are scarce because
162 the zone is extensively cultivated, and there is no significant relief due to the low dip of
163 the layers and the outcropping marls. In the northern part, however, fluvial incision
164 allows us to observe tilted Tortonian-Messinian calcarenites (Fig. 3A). Thus, folds
165 probably do not propagate through these regions and affect only the southwestern part
166 of the Depression.

167 The Salinas Fold is the major structure observed in the whole Depression. It is a
168 NNE-SSW box shaped antiform with a two-kilometre-wide crest. The dip of the flanks
169 (Figs. 2, 3 and 4) increases sharply, from 20° to 70°. This feature produces straight
170 boundaries in the topographic intersection that are not related to large NE-SW normal
171 faults, as suggested by previous authors (Serrano, 1979). The antiform culmination is
172 essentially flat, with dips lower than 20°. Therefore, the geometry of the fold could be
173 described as a box-fold without vergence (Fig. 3B). Although previous authors
174 (Rodríguez-Fernández 1982) point to the local presence of some patches of Triassic
175 rocks cropping out in the core of the antiform, only Tortonian-Messinian calcarenites

176 from Setenil Formation and some patches of Messinian marls have been distinguished
177 in this study. Six cartographic folds could be described running parallel to the Salinas
178 Fold, constituting a fold set that deforms an area 6 km long and 8 km wide (Figs. 2 and
179 3B). In addition, it is possible to identify minor folds with metre wavelengths and the
180 same orientation as the Salinas antiform, approximately N30°E. Their geometry is open,
181 with flanks dipping around 15-20°. These minor folds are fundamentally located in the
182 crest zone of the Salinas Fold and deform the calcarenites of Setenil Formation. It is not
183 possible to determine if they also deform the Late Messinian Limestone Member of the
184 Setenil Formation, because there are scarce outcrops of these rocks, and in all of them a
185 10° southeastward dip is observed.

186 The WNW-ESE Sierra de la Sanguijuela antiform (Fig. 2), situated SW of the
187 Salinas Fold, is parallel to the southwestern border of the Depression. Its shape
188 resembles that of the Salinas antiform and could be considered as the prolongation of
189 this fold, given that there are no interference structures between the two, although there
190 is a sharp change in fold axis orientation. There are no minor antiforms parallel to the
191 Sanguijuela antiform, in contrast to the Salinas one. On both sides of these folds there
192 are two synforms with the same orientation, NE-SW in the Salinas sector and WNW-
193 ESE in the Sanguijuela sector (Fig. 2 and 3B). Marls belonging to the Mina Formation
194 crop out in the core of these synforms.

195 The most recent rocks deformed by the kilometre scale box-folds are Tortonian-
196 Messinian calcarenites. The Depression contains no Pliocene deposits and the
197 Quaternary sediments are limited to non-deformed river channels. Although it is not
198 possible to determine the cessation of activity of these folds, field observations indicate
199 that both types of folding were simultaneously active in Late Tortonian to Late
200 Messinian times.

201

202 GRAVITY ANOMALY AND DEEP STRUCTURE

203 A new gravity survey was performed in the Ronda Depression in order to
204 determine the sedimentary thickness and the deep geometry and nature of its basement.
205 Data were acquired along several profiles covering all the sedimentary infill and the
206 Depression boundaries. Measurement stations along profiles were spaced at an average
207 of 250 m. Gravity data were acquired using a Master Worden gravimeter, with a
208 maximum accuracy of 0.01 mGal. The measurement sites were located with an e-trex
209 Garmin GPS and a barometric altimeter with 0.5 m altitude precision. The
210 measurements were referenced to a base station of the I.G.N. national gravimetric
211 network, located in Málaga, in order to calculate the absolute gravity value. Data
212 acquisition was carried out in cycles of less than three hours in order to correct
213 accurately the instrumental drift, tide variations and barometric changes. Topographic
214 corrections were done using a digital terrain model with a grid of 10 m of cell size for
215 the first 1600 m, and 200 m thereafter, to a total distance of 22 km. The Bouguer
216 anomaly was calculated taking into account a standard density ($d= 2670 \text{ kg/m}^3$) similar
217 to the density of the Subbetic rocks that form the basement.

218 The heterogeneous basement lithology (and therefore density) of the region
219 made it impossible to isolate the residual anomaly associated with the Neogene
220 sedimentary infill of the Ronda Depression, and therefore constrain its thickness. At the
221 southern boundary the basement is formed by Subbetic limestones with a high density
222 contrast, whereas the northern basement comprises Triassic rocks and Flysch units with
223 density values that are similar to or lower than the sedimentary infill.

224 In the Bouguer anomaly map 1:1.000.000 (I.G.N., 1976) (Fig. 5.A.), values in
225 the southern part of the Ronda Depression increase progressively to the SE. However, in

226 the western and northern parts, the isolines have a N-S direction, and anomaly values
227 increase gradually to the W. Changes in the direction of the regional anomaly signalled
228 by this Bouguer anomaly map are probably related to the deep crustal structure and
229 make it impossible to distinguish the anomaly related to the basement heterogeneities
230 and the variations in thickness of sedimentary infill. Therefore, a 2D model that
231 considers both sedimentary infill and shallow basement structures was made using the
232 Bouguer anomaly, with the GRAVMAG V.1.7. program of the British Geological
233 Survey (Pedley et al., 1993). A constant regional anomaly value due to the deep crustal
234 structures was taken into account.

235 The main features of the detailed Bouguer anomaly map of the Ronda
236 Depression (Fig. 5B) are two marked gravity minima observed in the middle and
237 northwestern parts of the depression. The southernmost one is elongated in NE-SW
238 orientation and reaches values of -88 mGal, while the minimum placed to the north
239 reaches -78 mGal. These minima are not detected in the regional gravity map of Spain
240 1:1.000.000 (I.G.N., 1976; Fig.5.A.) due to its scale and to the large distance between
241 measurements. There is a good correlation between the southernmost minimum and the
242 main structures of the Ronda Depression.

243 In sedimentary basins, minima are generally related to depocentres located on
244 synformal structures. Yet the correlation of the Bouguer gravity minima with the
245 Depression's major structures evidences that the southernmost minimum is over the
246 Salinas antiform, which is the main antiform of the Depression (Fig.5.B.). In some cases
247 gravity minima could also be related to ancient depocentres that are inverted. However,
248 this is not the situation in the Ronda Depression, where the lower parts of the
249 sedimentary sequence are located in the core of the antiform. In other words, the gravity

250 anomaly in this region allows us to determine the basement structure of the depression,
251 but does not enable us to estimate accurately the sedimentary infill geometry.

252 In order to integrate the surface geological data, a NW-SE gravity model
253 orthogonal to the main NE-SW folds was developed (Fig. 5C). The average density
254 assigned to each geological unit is related to the main lithology observed in the field
255 according to Telford et al. (1990): 2300 kg/m³ for the sedimentary infill, 2670 kg/m³ for
256 the Subbetic limestones, 2350 kg/m³ for the Flysch sandstones, and 2000 kg/m³ for the
257 Triassic marls with gypsum. The anomaly values change gradually, with no sharp
258 variations at the boundaries of the sedimentary infilling. This fact, together with the
259 surface geological data, suggests that the borders of the depression are unconformities
260 and are not related with high angle faults. In the southern part of the Depression, the
261 Neogene sediments lie over Subbetic units with a continuous NE-SW structure.
262 However, northwest of the Salinas fold, the basement has a chaotic structure and there
263 are kilometre scale limestone blocks included in a Triassic matrix.

264 The thickness of the Neogene sedimentary infill is irregular and may attain 300
265 m according to the geological data and the gravity modelling, although this cannot be
266 proved because there are no clearly related residual anomalies. Moreover, the thickness
267 of Triassic rocks located at the base of the model cannot be established accurately due
268 to the lack of other geophysical data such as well logs or seismic profiles. However, it is
269 possible to determine the areas where these rocks are close to the surface and their
270 geometry. The gravity method can provide evidence of lateral contrasts in density, but
271 not the vertical contrast, as horizontal layers whose effect is a constant regional level
272 may be overprinted upon regional anomalies.

273

274 DISCUSSION

275 In neotectonic studies, the precise dating of structures is essential for elucidating
276 the tectonic evolution of a region. The study of deformed intramontane sedimentary
277 basins is especially interesting, because it allows for precise estimations of the age of
278 recent tectonic structures. However, it is necessary to establish the mechanisms of
279 deformation in order to distinguish regional tectonic structures from local reactivations
280 that may lead to erroneous interpretations. In this way, the development of orthogonal
281 oriented structures, such as folds, should be analysed in detail in order to determine
282 their simultaneous development in a deformation stage, or the overprinting that would
283 provide evidence of two regional deformation stages. The presence of low density rocks
284 at depth is the main mechanism responsible for reactivation of earlier structures through
285 salt tectonics involving only local deformations. The Ronda Depression, affected by
286 irregularly distributed orthogonal folds, provides a good opportunity to investigate the
287 late development of folds and to discuss the implications thereof.

288 In the Western Betics, a main part of the brittle and ductile deformation of the
289 outcropping tectonic units took place before Tortonian, as rocks of Late Miocene age lie
290 unconformably over the deformed External Zones and Flysch Units. In addition,
291 deformation in these Late Miocene rocks is local and generally of low intensity,
292 consisting of tilting, gentle folds and very scarce faults with small displacements. The
293 NE-SW fold-and-thrust belt that determines the structure of the Subbetic basement (Fig.
294 6A) was developed in a post-Early Burdigalian deformation event (Crespo-Blanc and
295 Campos, 2001; Pérez-López and Pérez Valera, 2007; Crespo-Blanc, 2008). In this stage,
296 accompanied by regional NW-SE compression due to the Eurasian-African plate
297 convergence, low density rocks were differentially accumulated at the core of the
298 antiformal structures.

299 Gravity data acquired in the Depression allow us to discern the different nature
300 of the basement beneath the current Neogene sedimentary succession. This fact
301 conditions the heterogeneous distribution of the folds deforming the Late Miocene
302 infill. Subbetic limestones are identified continuously from the southern border of the
303 Depression up to its central part. In addition, northwards of the Salinas antiform, large
304 kilometre scale blocks of high density (Fig. 5C) are attributed to Jurassic limestones of
305 the Subbetic units, which may represent the Subbetic Chaotic Complexes. Bouguer
306 gravity minima point to areas of accumulation and the shallow position of the low
307 density Triassic rocks. These minima have NE-SW elongated shapes (Fig. 5B), similar
308 to the trend of the folds that deform the surrounding basement and the southern part of
309 the Depression. In the northwestern minimum, the gravity model suggests that Triassic
310 rocks are located directly under the undeformed sedimentary infill. However, the
311 southeastern minimum coincides with the core of the Las Salinas antiform (Fig. 5B and
312 C), suggesting that low density rocks were related to the fold development.

313 During Late Tortonian-Late Messinian, marine sediments of the Ronda
314 Depression were deposited in a progressive unconformity (Rodríguez-Fernández, 1982)
315 over the Salinas antiform due to the interference of sedimentation, erosion, and tectonic
316 processes (Fig. 6B). The development of box-fold geometries could be the consequence
317 of remobilization and uplift of previous thick Triassic rock accumulations (Fig. 6C)
318 simultaneous with the uplift of the Betic Cordillera and the transition from marine to
319 continental sedimentation. Other factors are needed to develop this type of fold in
320 compressional settings, as has been established using analogue models (Bonini, 2003):
321 the load due to the overlying sedimentary sequence, the presence of fluids and, indeed, a
322 sharp inversion of density in the sedimentary sequence. The combination of these
323 factors may condition the fold type: from type 1 (Bonini, 2003) localized above a thrust

324 up to type 2, formed in front of the most external thrust. The development of box fold
325 geometries, as the Salinas-Sanguijuela antiform, is a transitional situation between these
326 cases.

327 Previous studies (Serrano 1979) have proposed a strictly diapiric origin of the
328 Salinas fold controlled by the presence of ductile Triassic rocks in its core. In any case,
329 the previous tectonic setting would have conditioned an early NE-SW elongated
330 accumulation of low-density rocks that determined the late reactivation of the fold. This
331 setting, where the fold orientation is inherited, may then be analysed to understand the
332 local deformations, but cannot be used to determine recent regional deformation stages.

333 The salt tectonics that occurred during the reactivation of the Salinas antiform
334 may be responsible for its geometry and location, featuring sharp boundaries, box-fold
335 shape without predominant vergence, and restricted deformation in the southeastern part
336 of the depression. The orthogonal development of the Sanguijuela fold was produced
337 roughly simultaneously to the formation of the Salinas fold. Both folds are connected
338 along an area of highly curved crest line showing none of the typical dome-and-basin
339 interference structures that are generally seen in orthogonal trending folds. The sharp
340 change in orientation in the southern part of the Depression may be due to the WNW-
341 ESE thick, rigid limestones of the southwestern boundary of the depression. The late
342 folds do not propagate outside the depression. The competent folded upper layer, made
343 up of the Jurassic limestones and Neogene sedimentary infill, accommodates the
344 southward pushing of the Las Salinas antiform by the development of the La
345 Sanguijuela antiform. Similar examples of fold development related to a high
346 accumulation of ductile Triassic rocks have been described by other authors in the Betic
347 Cordillera (López-Garrido and Vera, 1974).

348 The slightly deformed and unconformable Neogene sedimentary infill in the
349 Western Betic Cordillera suggests that the deformation is concentrated largely in
350 correspondence of deep rooted structures that only affect the frontal part. Piggy-back
351 basins like the Ronda Depression mainly underwent northwestward transport and uplift.
352 Crespo-Blanc and Campos (2001) considered the late folds to be open, deforming the
353 thrust planes that affect the basement of the depression. However, the continuity of the
354 folds affecting the surrounding basement with the folds observed in the Late Miocene
355 infill is not well constrained, and probably does not occur because field observations
356 give no evidence that the basal unconformity has been affected by these structures in the
357 basin boundaries. Thus, folds of the Late Miocene sedimentary infill are local, restricted
358 to the Ronda Depression and may not be used to date the regional deformation stages.

359

360 CONCLUSIONS

361 A detailed study of the Ronda Depression, including field geological and gravity
362 observations, has provided some insights for analysis of fold reactivation in a
363 framework of heterogeneity of the basement and sedimentary infill. An early
364 deformation stage during NW-SE African and Eurasian plate convergence affected the
365 basement during Early and Middle Miocene times and produced a NE-SW oriented
366 fold-and-thrust belt. During this stage, the accumulation of ductile low density Triassic
367 rocks, belonging to the Subbetic sequence, took place in the core of NW vergent folds.
368 Since the Late Miocene, the Ronda Depression may be considered a northward-moving
369 piggy-back basin, having experienced uplift, evidenced by the elevation of the
370 unconformable Tortonian-Messinian marine sediments, but scarce tectonic deformation.
371 The remobilization of this inherited and heterogeneous distribution of Triassic rocks is
372 evidenced by Bouguer gravity minima. The accumulation of low density basement

373 rocks controlled the development of the Salinas box-shaped antiform, while the
374 simultaneously developed orthogonal Sanguijuela fold is determined by the competent
375 southern border of the basin.

376 Reactivation of basement folds by diapirism is one of the main mechanisms of
377 deformation of the sedimentary infill placed above low density basement rocks.
378 Although reactivated folds are generally elongated and may be interpreted as a
379 consequence of a new regional tectonic compressive deformation stage, several features
380 may be considered as evidence of the different mechanisms at work during their origin:
381 heterogeneous fold distribution; no dominant vergence and mostly box geometries.
382 Furthermore, this setting can give rise to the simultaneous development of folds with
383 orthogonal axes. These recent folds are formed by salt tectonics and should be analysed
384 with caution, as has been done in the Ronda Depression, because they document local
385 deformation stages only.

386

387

388 ACKNOWLEDGEMENTS

389 This study was supported by a PhD grant to the first author from Spain's Ministerio de
390 Educación y Ciencia and the projects CSD2006-00041 and CGL 2006-06001 (MEC)
391 and Junta de Andalucía.

392

393 REFERENCES

- 394 Bonini, M., 2003. Detachment folding, fold amplification, and diapirism in thrust wedge
395 experiments. *Tectonics* 22.
- 396 Calaforra, J.M., Pulido-Bosch, A., 1999. Gypsum karst features as evidence of diapiric
397 processes in the Betic Cordillera, Southern Spain. *Geomorphology* 29, 251–264.

- 398 Callot, J.P., Jahani S., Letouzey, J., 2006. The Role of Pre-Existing Diapirs in Fold and
399 Thrust Belt Development. In: Lacombe O, Roure F, Lavé J, Vergés J (ed) Thrust Belts
400 and Foreland Basins, pp 309-325.
- 401 Caritg, S., Burkhard, M., Ducommun, R., Helg, U., Kopp, L., Sue, C., 2003. Fold
402 interference patterns in the Late Palaeozoic Anti-Atlas belt of Morocco. *Terra Nova* 16,
403 27–37.
- 404 Crespo-Blanc, A., 2007. Superimposed folding and oblique structures in the
405 palaeomargin-derived units of the Central Betics (SW Spain). *Journal of the Geological*
406 *Society London* 164, 621–636.
- 407 Crespo-Blanc, A., 2008. Recess drawn by the internal zone outer boundary and oblique
408 structures in the paleomargin-derived units (Subbetic Domain, central Betics): An
409 analogue modelling approach. *Journal of Structural Geology* 30, 65-80.
- 410 Crespo-Blanc, A. and Campos, J. 2001. Structure and Kinematics of the South Iberian
411 paleomargin and its relationship with the Flysch Trough units; extensional tectonics
412 within the Gibraltar Arc fold-and thrust belt (western Betics). *Journal of Structural*
413 *Geology* 23, 1615-1630.
- 414 García-Tortosa, F.J., Sanz de Galdeano, C., Alfaro, P., Galindo Zaldívar, J., Peláez,
415 J.A., 2007. La falla y los pliegues de Galera. In: Sanz de Galdeano C, Peláez JA (ed.).
416 La cuenca de Guadix Baza. Estructura, tectónica activa, sismicidad, geomorfología y
417 dataciones existentes, 141-153.
- 418 Groupe de Recherche Néotectonique de l'Arc de Gibraltar, 1977. "L'histoire tectonique
419 récente (Tortonien a Quaternaire) de l'Arc de Gibraltar et des bordures de la mer
420 d'Alboran". *Bull. Soc. Géol. Fr.* 7, t. XIX.
- 421 I.G.N., 1976. Mapa de anomalías de Bouguer. Escala 1:1.000.000. I.G.N., Madrid.

- 422 Jallouli, C., Chikhaoui, M., Braham, A., Moncef Turk, M., Mickus, K., Benassi, R.,
423 2005. Evidence for Triassic salt domes in the Tunisian Atlas from gravity and geological
424 data. *Tectonophysics* 396, 209–225.
- 425 López-Garrido, A.C., Vera, J.A., 1974. Diapirismo reciente en la depresión de Guadix-
426 Baza (Sector del Negretín). *Estudios Geológicos* 30, 611-618.
- 427 Marín-Lechado, C., Galindo-Zaldívar, J., Rodríguez-Fernández, L.R., Pedrera, A.,
428 2007. Mountain Front Development by Folding and Crustal Thickening in the Internal
429 Zone of the Betic Cordillera-Alboran Sea Boundary. *Pure and Appl. Geophys.* 164, 1–
430 21.
- 431 Marques, F.O., Cobbold, P.R., 2006. Effects of topography on the curvature of fold-
432 and-thrust belts during shortening of a 2-layer model of continental lithosphere.
433 *Tectonophysics* 415, 65–80.
- 434 Mon, R., Monaldi, C.R., Salfity, J.A., 2005. Curved structures and interference fold
435 patterns associated with lateral ramps in the Eastern Cordillera, Central Andes of
436 Argentina. *Tectonophysics* 399, 173-179.
- 437 Morales, J., Vidal, F., De Miguel, F., Alguacil, G., Posadas, A.M., Ibáñez, J.M.,
438 Guzmán, A., Guirao, J.M., 1990. Basement structure of the Granada basin, Betic
439 Cordilleras, Southern Spain. *Tectonophysics* 171, 337-348.
- 440 Nilforoushan, F., Koyi, H.A., 2007. Displacement fields and finite strains in a sandbox
441 model simulating a fold-thrust-belt. *Geophys. J. Int.* 169, 1341–1355.
- 442 Pedley, R.C., Busby, J.P., Dabeck, Z.K., 1993. GRAVMAG User Manual- Interactive
443 2.5D gravity and magnetic modelling. British Geological Survey, Technical Report
444 WK/93/26/R.
- 445 Pedrera, A., Galindo-Zaldívar, J., Sanz de Galdeano, C., and López Garrido, A.C.,
446 2007. Fold and fault interactions during the development of an elongated narrow basin,

- 447 The Almanzora Neogene-Quaternary Corridor (SE Betic Cordillera, Spain). *Tectonics*
448 26.
- 449 Pérez-López, A., Pérez-Valera, F., 2003. El diapirismo como factor principal de la
450 resedimentación de las rocas del Triásico durante el Terciario en las Zonas Externas de
451 la Cordillera Bética. *Geotemas* 5, 189-193.
- 452 Pérez-López, A., Sanz de Galdeano, C., 1994. Tectónica de los materiales triásicos en el
453 sector central de la Zona Subbética (Cordillera Bética). *Rev. Soc. Geol. Esp.* 7, 141-153
- 454 Pinto, V., Casas, A., Rivero, L., Torné, M., 2005. 3D gravity modeling of the Triassic
455 salt diapirs of the Cubeta Alavesa (northern Spain). *Tectonophysics* 405, 65– 75.
- 456 Platt, J., Allerton, S., Kirker, A., Platzman, E., 1995. Origin of the western Subbetic arc
457 (South Spain), palaeomagnetic and structural evidence. *Journal of Structural Geology*
458 12, 765-775.
- 459 Platzman, E.S., 1992. Paleomagnetic rotations and the kinematics of the Gibraltar Arc.
460 *Geology* 20, 311-314.
- 461 Rodríguez-Fernández, J., 1982. El Mioceno del sector central de las Cordilleras Béticas.
462 Tesis Doctoral Universidad de Granada, pp 224.
- 463 Rodríguez-Fernández, J. and Sanz de Galdeano, C., 2006. *Basin Research* 18, 85-102.
- 464 Roldán, F.J., 1995. Evolución neógena de la Cuenca del Guadalquivir. Tesis Doctoral,
465 Univ. De Granada, pp 259.
- 466 Ruano, P., Galindo-Zaldívar, J., Jabaloy, A. 2004. Recent Tectonic Structures in a
467 Transect of the Central Betic Cordillera. *Pure Appl. Geophys.* 161, 541–563.
- 468 Sanz de Galdeano, C., Vera, J.A., 1992. Stratigraphic record and palaeogeographical
469 context of the Neogene basins in the Betic Cordillera, Spain. *Basin Research* 4,21-36.
- 470 Sanz de Galdeano, C., Galindo-Zaldívar, J., López Garrido, A.C., Alfaro, P., Pérez-
471 Valera, F., Pérez-López, A., García Tortosa, F.J., 2006. La falla de Tíscar: Su

472 significado en la terminación sudoeste del arco Prebético. Rev. Soc. Geol. España 19,
473 271-280.

474 Sanz de Galdeano, C., Delgado, J., Galindo-Zaldívar, J., Marín-Lechado, C., Alfaro, P.,
475 García Tortosa, F.J., 2007. Principales rasgos geológicos deducidos a partir de los
476 mapas gravimétricos de la cuenca de Guadix-Baza. In: Sanz de Galdeano C, Peláez JA
477 (ed) La cuenca de Guadix Baza. Estructura, tectónica activa, sismicidad, geomorfología
478 y dataciones existentes, pp 101-110.

479 Serrano, F., 1979. Los foraminíferos planctónicos del Mioceno superior de la cuenca de
480 Ronda y su comparación con los de otras áreas de la Cordilleras Béticas. Tesis Doctoral.
481 Facultad de Ciencias. Universidad de Málaga, pp 272.

482 Telford, W.M., Geldart, L.P., Sheriff, R.E., 1990. Applied Geophysics. Cambridge
483 University press, pp 770.

484 Viseras, C., Soria, J.M., Fernández, J., 2004. Cuencas neógenas postorogénicas de la
485 Cordillera Bética. In: Vera (ed) Geología de España. SGE – IGME, pp 576-581.

486
487 FIGURES

488

489 Figure 1. Geological setting of the Ronda Depression in the framework of the Betic and
490 Rif Cordillera.

491 Figure 2. Tectonic sketch of the Ronda Depression. Cross sections of Fig. 3 and gravity
492 profile of Fig. 5c are indicated. UTM coordinates are in kilometres.

493 Figure 3. Geological NW-SE cross-sections of the Ronda Depression. The position of
494 the cross-sections is marked in Fig. 2. Gravity data have been qualitatively taken into
495 account to constraint the deep structure. The legend is the same as in Fig. 2.

496 Figure 4. Panoramic view and orthophoto image of the Salinas Antiform. Photographs
497 show the high dip of the flanks in this box fold.

498 Figure 5. Bouguer anomalies and gravity model: a. Bouguer anomaly map of Betic
499 Cordillera 1:1.000.000 (I.G.N. 1976); b. Bouguer anomaly map of Ronda Depression.
500 The modelled profile and the axial traces of the folds are drawn (in grey: minor open
501 folds; in white: Salinas and Sanguijuela folds); c. 2D NW-SE gravity model.

502 Figure 6. Tectonic evolution sketch of fold reactivation in the Ronda Depression. a)
503 Post-Early Burdigalian deformation event that determines the structure of the Subbetic
504 due to the NW-SE Eurasian-African plate convergence; b) During Late Tortonian-Late
505 Messinian, marine sediments of the Ronda Depression were deposited in a progressive
506 unconformity; c) Since Late Tortonian, remobilization and uplift of previous thick
507 Triassic rock accumulations simultaneous to the uplift of the Betic Cordillera.

508

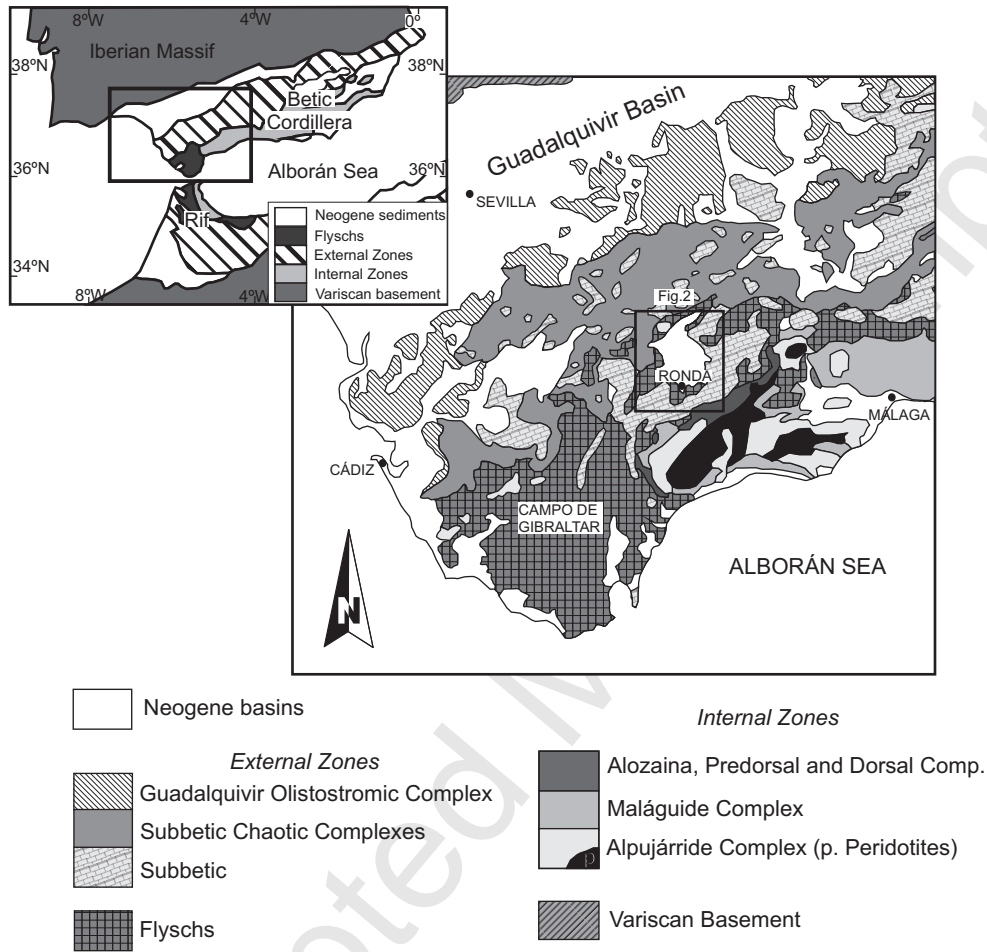


Fig.1 Ruiz-Constán et al.

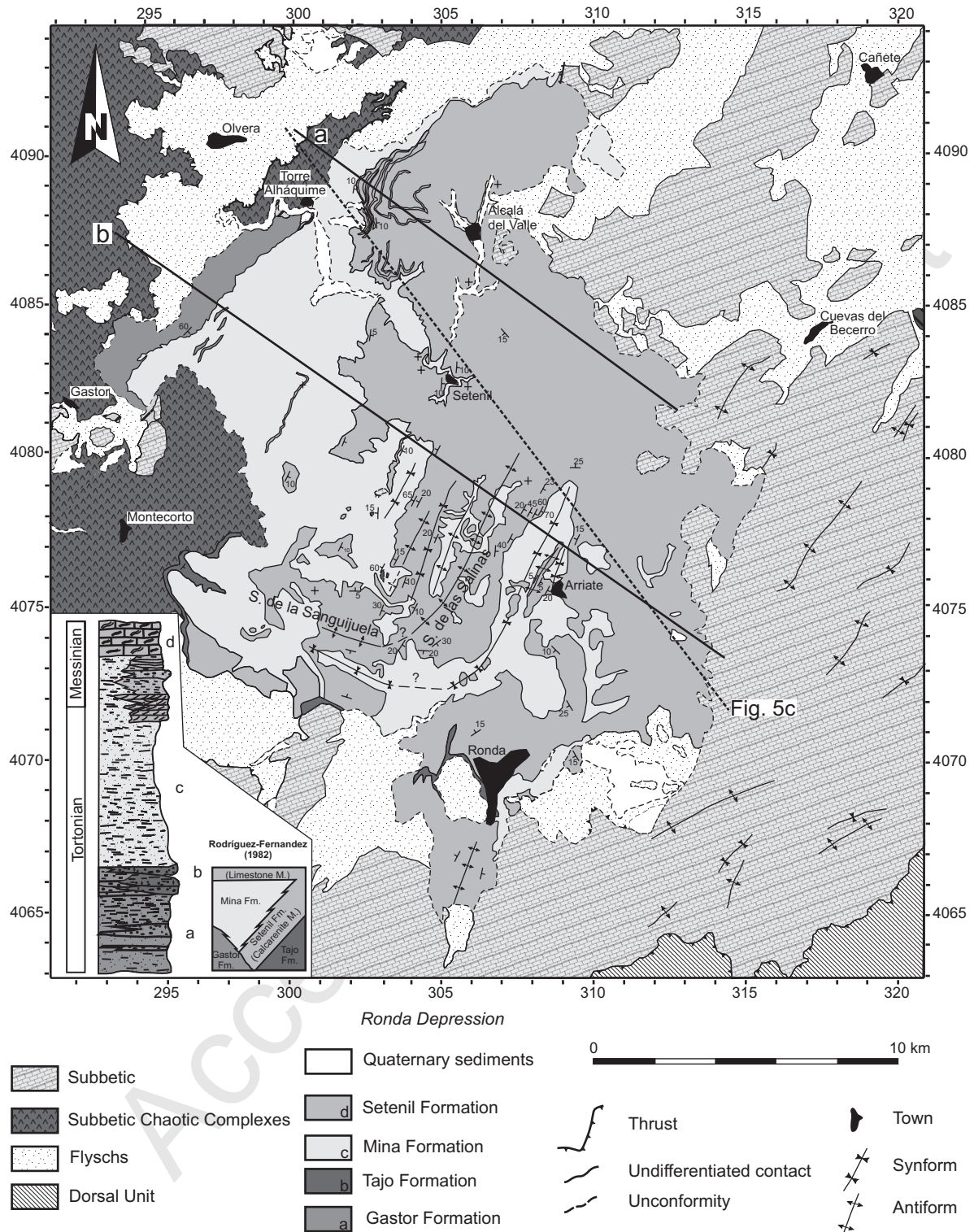


Fig.2 Ruiz-Constán et al.

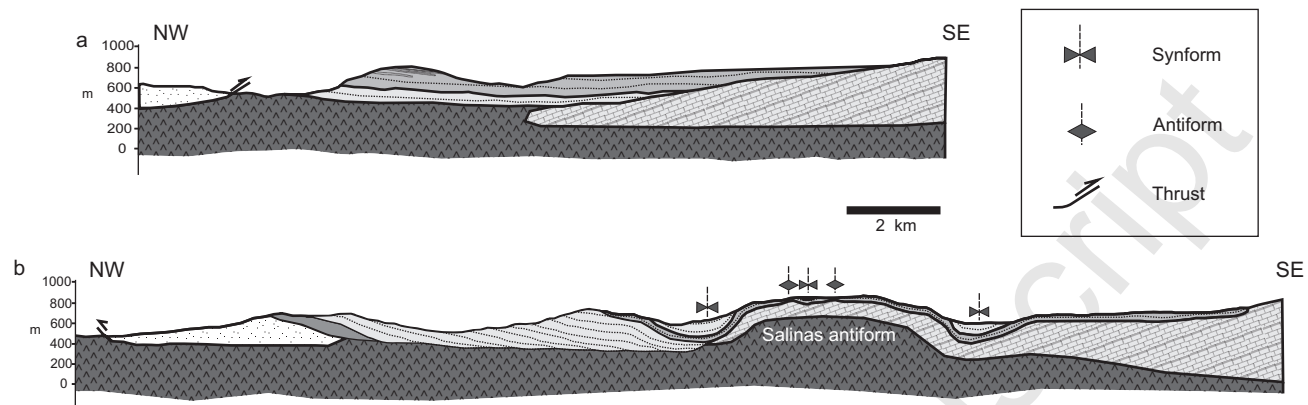


Fig.3 Ruiz-Constán et al.

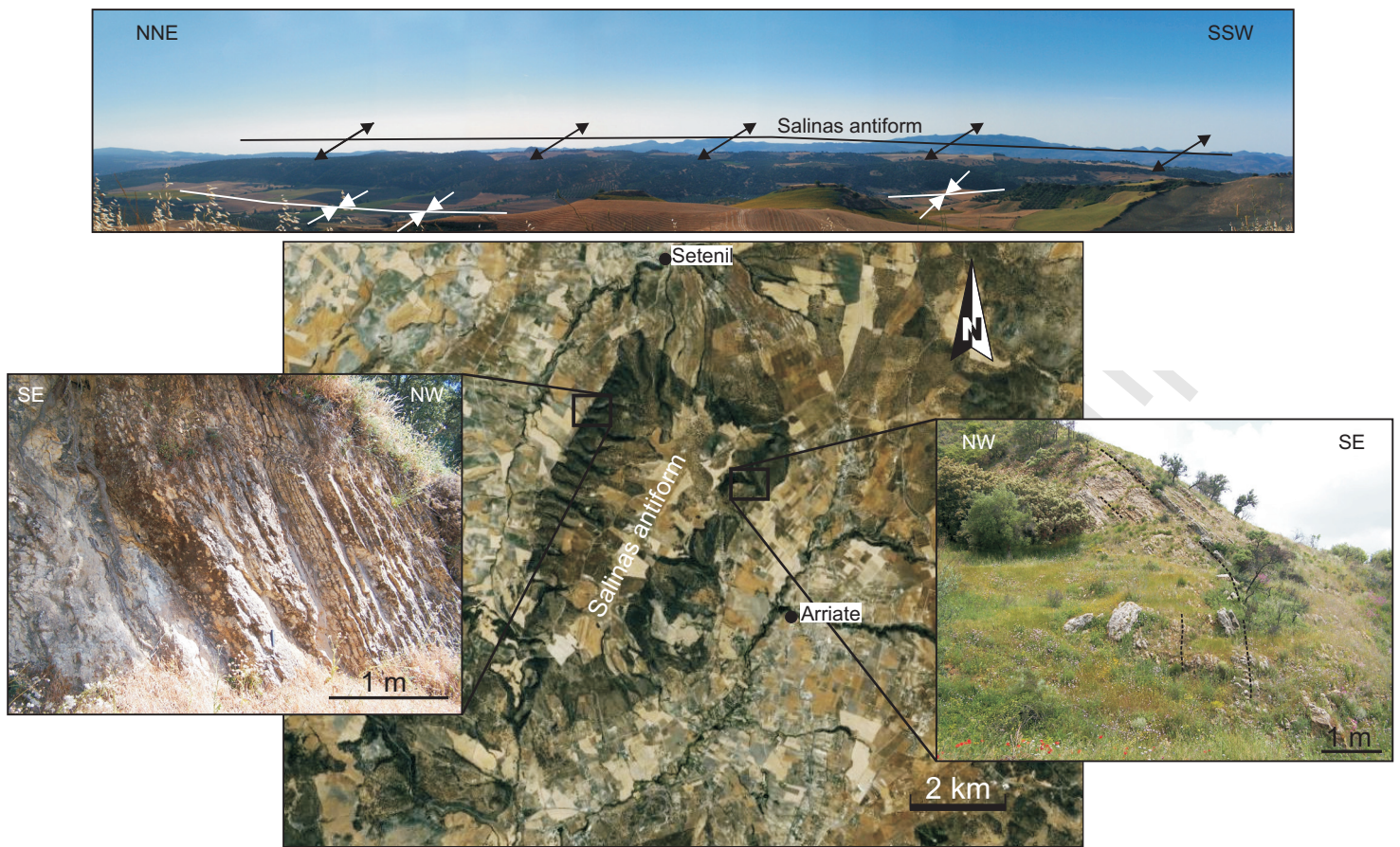


Fig 4. Ruiz-Constán et al.

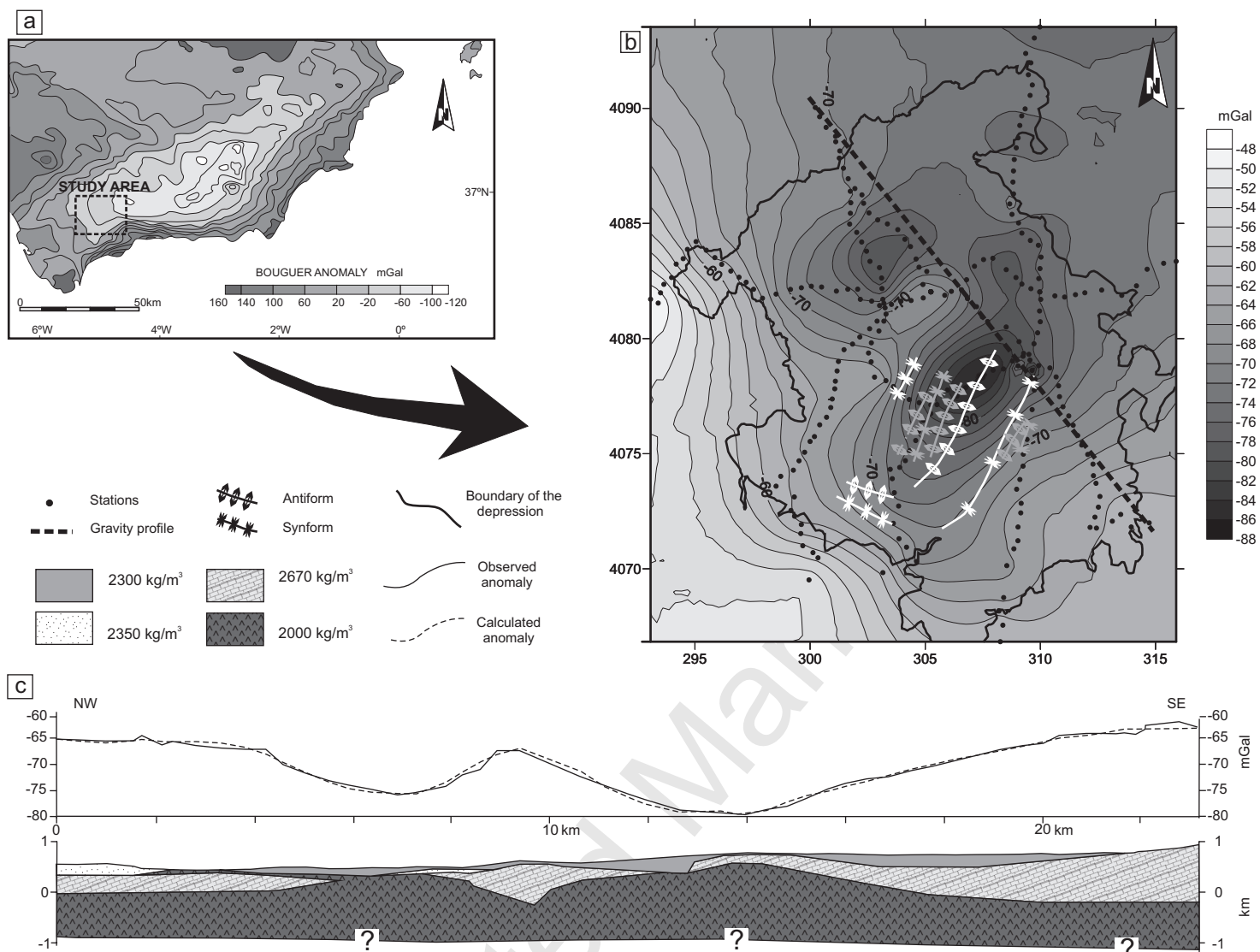


Fig.5 Ruiz-Constán et al.

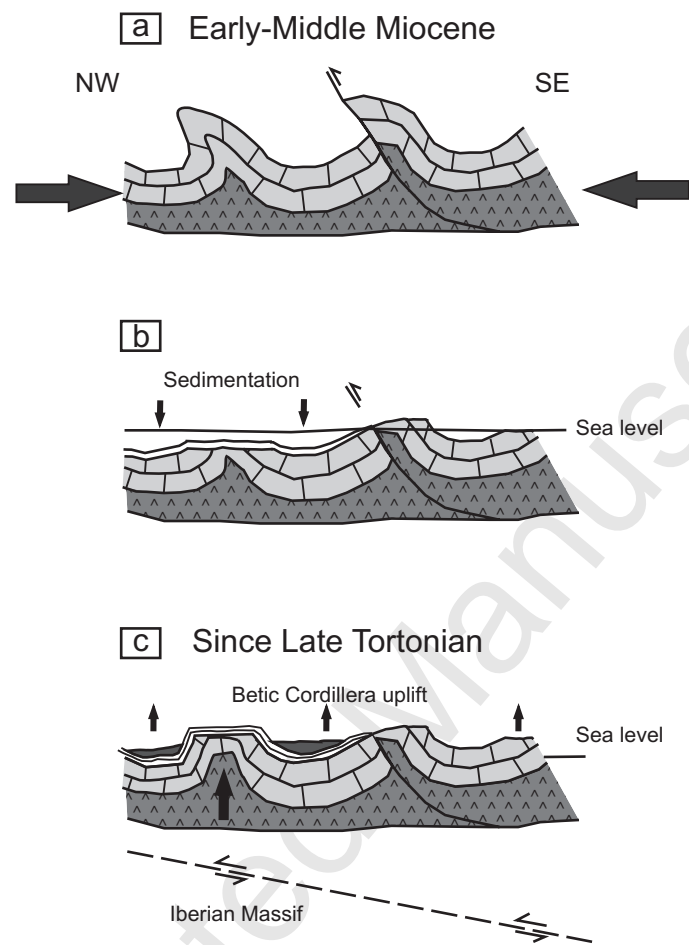


Fig6. Ruiz-Constán et al.